Sticking Probability on Zeolites

ARTICLE *in* THE JOURNAL OF PHYSICAL CHEMISTRY B · AUGUST 2005

Impact Factor: 3.3 · DOI: 10.1021/jp0511606 · Source: PubMed

4 AUTHORS, INCLUDING:

Jean-Marc Simon
University of Burgundy
83 PUBLICATIONS **676** CITATIONS
SEE PROFILE

Jean-Pierre Bellat
University of Burgundy
111 PUBLICATIONS **1,162** CITATIONS
SEE PROFILE

Sticking Probability on Zeolites

Jean-Marc Simon,[†] Jean-Pierre Bellat,[†] Sergey Vasenkov,[‡] and Jörg Kärger*[,‡]

Laboratoire de Recherches sur la Réactivité des Solides, UMR 5613, Université de Bourgogne-CNRS, 9, Avenue Savary, BP 47870, 21078 Dijon Cedex, France, and Institut für Experimentelle Physik I, Universität Leipzig, Linnéstrasse 5, D-04103 Leipzig, Germany

Received: March 7, 2005; In Final Form: May 24, 2005

The sticking coefficient, i.e., the probability that, on hitting the surface of a nanoporous particle (zeolite), a molecule shall be able to enter the intracrystalline space, is a key quantity for the application of such materials in heterogeneous catalysis and molecular sieving. On the basis of pulsed field gradient NMR diffusion measurements and molecular dynamics simulations, typical values of this probability are found to be close to one. They exceed previous estimates on the basis of IR uptake measurements by many orders of magnitude.

1. Introduction

In their main fields of application, such as mass separation and heterogeneous catalysis,[1−3] in addition to mass transfer resistances in the intra- and interparticle spaces the functionality of nanoporous materials notably depends on how fast the molecules encountering the outer surface of the particles are able to penetrate into their interior. For a quantitation of this process one may introduce, in compleate analogy to its classical definition,[4] a sticking coefficient. It represents the probability that, on encountering the particle surface, a molecule will be captured by the particle and will enter its intraparticle space, rather than being rejected to continue its trajectory in the space between the particles. In addition to its practical relevance for the performance of nanoporous materials in separation and catalysis, the sticking coefficient represents a fundamental quantity of molecular dynamics on interfaces.

Originally, the sticking coefficient has been introduced as a measure of the probability that a molecule colliding with a plane surface will be captured by it.[4] Experimental studies include hydrogen, nitrogen, oxygen, carbon monoxide, and ethylene as probe molecules and a large spectrum of metals and metal oxides as targets[5] with sticking coefficients typically between 0.1 and 1. Most recently, the sticking probability of such systems (nitrogen onto GaN surfaces) has also been the subject of molecular dynamics (MD) simulations.[6]

Considering, e.g., argon, water, and methanol, MD simulations have also been performed for the elementary process of molecular transition from the gaseous phase into the liquid phase.[7−10] Also in these studies the sticking probabilities ("condensation coefficients") were found to be close to 1.

In contrast to the rather substantial literature devoted to the sticking probabilities in these two types of systems, to the best of our knowledge, so far only in ref 11 is an estimate of the sticking probability of molecules colliding with the surface of nanoporous solids given. This estimate was based on the measurement of the rate of the intensity increase of the respective IR bands in uptake measurements with toluene on the MFI-type zeolite.[11] Comparing the actual uptake with the total amount of collisions of the gas phase molecules with the zeolite surface as resulting from kinetic gas theory, it followed that only after 1 out of 10^7 collisions did a molecule pass from the gas phase into the zeolite pore volume. Since in many cases uptake measurements are well known to be limited by "external" process like transport through the bed of particles (long-range diffusion) or heat release,[1,12] the sticking coefficient of 10^{-7}, as resulting from this estimate, cannot be considered to be more than a lower limit.

In the present study, we have followed two independent and completely different routes to determine molecular sticking coefficients on nanoporous solids. As a first option, we have analyzed the patterns of molecular transportation for displacements notably exceeding the diameters of the individual nanoporous particles as accessible by the pulsed field gradient (PFG) NMR method.[12−16] Second, we have deduced the sticking probability from MD simulations[17,18] involving molecular exchange between a nanoporous host system and the surrounding atmosphere.[19] Both routes shall be shown to lead to estimates of coinciding orders of magnitude, which, moreover, comply to a much better extent with the range of sticking coefficients on flat surfaces and on liquid-vapor interfaces[20] than do the first estimates for zeolitic host−guest systems as provided by ref 11.

2. Evidence by Pulsed Field Gradient NMR

The quantity directly accessible by the pulsed field gradient (PFG) NMR technique is the so-called propagator $P(x,t)$.[12−14,21,22] It denotes the probability density that during time t an arbitrarily selected molecule within the system under study is shifted over a distance x in the direction of the applied field gradient. In the case of normal diffusion, it holds that

$$P(x,t) = (4\pi Dt)^{-1/2} \exp\left(-\frac{x^2}{4Dt}\right) \quad (1)$$

where D denotes the self-diffusivity. Equation 1 results as the solution of the diffusion equation (Fick's second law)

$$\partial c/\partial t = D\partial^2 c/\partial x^2 \quad (2)$$

for the initial condition $c(x,t=0) = \delta(x)$.[12−14] With eq 1, the mean square displacement (i.e., the variance (width) of the

* Corresponding author. E-mail: kaerger@physik.uni-leipzig.de. Phone +49 341 97 32502. FAX +49 341 97 32549.
† Université de Bourgogne-CNRS.
‡ Universität Leipzig.

10.1021/jp0511606 CCC: $30.25
Published on Web 06/23/2005

distribution) results to be

$$\langle x^2(t)\rangle = \int x^2 P(x,t)\,\mathrm{d}x = 2Dt \tag{3}$$

Alternatively, eqs 1 and 3 may be considered to be an immediate consequence of the central limit theorem of statistics.[23] It indicates that the probability distribution of molecular displacements is a Gaussian with a mean square displacement increasing linearly with time. As a necessary and sufficient condition, it has to be implied that the observation time t may be subdivided into a sufficiently large number of time intervals, so that the probability distribution of molecular displacement during each of these time intervals is identical and independent of the past. In the diffusion context, these time intervals are represented by the molecular mean lifetimes in the unit space element to which the respective diffusion mode is referred.

The primary quantity measured by PFG NMR is the intensity of the NMR signal, the so-called spin−echo, observed under the application of a suitably chosen sequence of pulses of an additional, inhomogeneous magnetic field, the "field gradient pulses". This spin−echo intensity is found to decay with increasing intensity of the field gradient pulses following the relation[12−14]

$$\Psi(t,\gamma\delta g) = \int P(x,t)\cos(x\gamma\delta g)\,\mathrm{d}x \tag{4}$$

where the x coordinate represents the direction of the pulsed field gradient, γ stands for the gyromagnetic ratio, and t, δ, and g denote the separation, width, and intensity of the field gradient pulses. With eq 1, i.e., under the conditions of normal diffusion, from eq 4 the relation for the PFG NMR spin−echo attenuation results to be

$$\Psi(t,\gamma\delta g) = \exp(-\gamma^2\delta^2 g^2 Dt) \tag{5}$$

which, by means of eq 3, may be transferred into

$$\Psi(t,\gamma\delta g) = \exp(-\gamma^2\delta^2 g^{2\langle x^2(t)\rangle}/2) \tag{6}$$

Equation 6 represents a good approximation for the spin−echo attenuation even under conditions where the propagator is not strictly given anymore by a Gaussian.[12−14]

On applying PFG NMR to studying molecular diffusion in beds of nanoporous particles (zeolite crystallites), one may distinguish between two limiting conditions of diffusion measurement where eq 5 is fulfilled, viz., the regimes of intracrystalline diffusion and of long-range diffusion.[12,24−26] They are defined by the requirement that molecular root-mean-square displacements $\langle x(t)\rangle^{1/2}$ are either much smaller (case of intracrystalline diffusion) or much larger (case of long-range diffusion) than the particle (crystallite) diameters. In both cases, to allow for such an interpretation, the space units in which the diffusion equation (eq 2) with the respective diffusivities is represented, have to be sufficiently small with respect to the total diffusion path. On the other side, they have to be at least comparable with the unit cell for the measurement of intracrystalline diffusion and with the crystal diameter for measuring under the regime of long-range diffusion. The schemes of the inserts to Figure 1 show an example of such a unit space element for the description of long-range diffusion. In both limiting cases, the propagator relevant for the diffusion measurement is a Gaussian as given by eq 1, with a diffusivity D referred to as the coefficient of intracrystalline or of long-range diffusion.

In the following we are going to demonstrate that the very fact of the observation of long-range diffusion by means of PFG NMR includes important information about the sticking probability of the molecules in the gaseous space between the individual nanoporous particles.

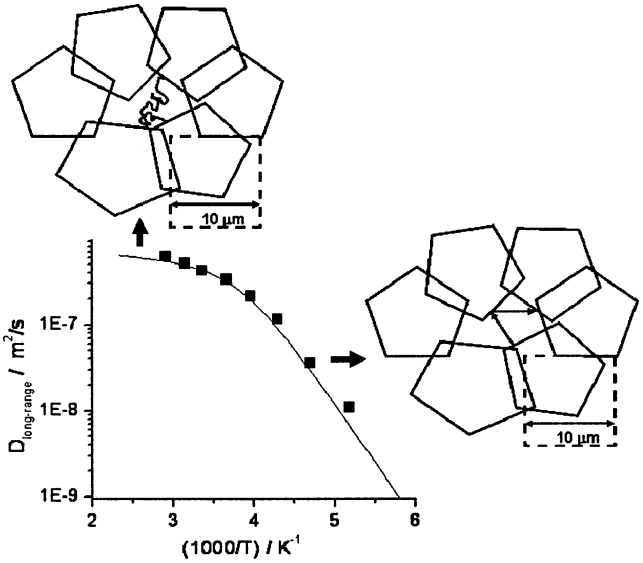

Figure 1. Temperature dependence of the coefficient of long-range self-diffusion of ethane measured by PFG NMR in a bed of crystallites of zeolite NaX and comparison with the theoretical estimate based on the sketched models of prevailing Knudsen diffusion (low temperatures, molecular trajectory consists of straight lines connecting the points of surface encounters) and gas-phase diffusion (high temperatures, mutual collisions of the molecules lead to the Brownian type of trajectories in the intercrystalline space).[16] The squares with broken lines represent the typical extension of a unit space element in the regime of long-range diffusion.

Let us at first review the main features of the well-established concept of PFG NMR measurements under the regime of long-range diffusion.[16,24,27−30] In many cases it is found to completely comply with Fick's laws of normal diffusion with a self-diffusivity

$$D_{\mathrm{long-range}} = p_{\mathrm{inter}} D_{\mathrm{inter}} \tag{7}$$

where p_{inter} and D_{inter} denote the fraction of molecules in the intercrystalline space and their diffusivity. The quantity p_{inter} may be easily determined from the adsorption isotherm and the particle bed density,[24−31] while the intercrystalline diffusivity may be represented by the gas-kinetic approach[12,16,24]

$$D_{\mathrm{inter}} = \frac{1}{3}\lambda_{\mathrm{eff}}\bar{u}/\eta \tag{8}$$

with λ_{eff}, $\bar{u}$, and η denoting, respectively, the effective mean free path and the mean thermal velocity of the molecules and the bed tortuosity. PFG NMR studies under the conditions of gas-phase adsorption are usually performed with fused sample tubes. Since the total amount adsorbed is much larger than the amount of molecules in the gas phase, p_{inter} is proportional to the pressure in the gas phase of the sample.

As an example, Figure 1 reproduces the long-range diffusivity data of ethane in a bed of crystallites of zeolite NaX communicated in ref 16. The Arrhenius plots of the long-range diffusivities exhibit two distinctly different dependencies. As illustrated by the inserts, they may be attributed to two different mechanisms of diffusion in the intercrystalline space, which prevail in different temperature ranges.

At sufficiently low temperatures the gas phase concentration is small enough so that the occurrence of mutual molecular

collisions in the intercrystalline space is negligibly small in comparison with molecular collisions with the outer surface of the zeolite crystallites. Under this condition, Knudsen diffusion is prevailing. As a consequence, the magnitude of the effective mean free path remains constant with varying temperature. Since, within one regime,[16] also the tortuosity is unaffected by temperature variation, according to eq 8 the temperature dependence of D_{inter} is given by that of the mean thermal velocity, which increases with only the square root of the temperature. This means that the temperature dependence of the long-range diffusivity is dominated by p_{inter}. Thus, owing to its proportionality with the gas-phase pressure, p_{inter}, and hence also $D_{long-range} = p_{inter}D_{inter}$, follows the Arrhenius dependence with an activation energy coinciding with the isosteric heat of adsorption.

With further increasing temperature, eventually the gas-phase concentration within the sample tube becomes high enough so that mutual collisions of the molecules in the intercrystalline space become relevant. Thus, under the now prevailing mechanism of gas-phase diffusion, the mean free path and hence D_{inter} decreases with increasing concentration. As a consequence, the increase of p_{inter} with increasing temperature is more and more compensated by the decrease of D_{inter}, caused by the reduced mean free path. In ref 16, this model was shown to lead to quantitative agreement with the measured long-range diffusivities over the complete temperature range.

For deducing information about the sticking probability of the molecules in the gas phase in the bed of nanoporous particles, the measured diffusion properties have to be discussed in an alternative and in fact novel way. As stated at the beginning of this section, long-range diffusion can appear only as a process of normal diffusion, i.e., as a phenomenon, governed by Fick's second law, if the total observation time may be divided into time intervals so that the probability functions of molecular propagation in subsequent time intervals and, hence, in the corresponding space elements, are uncorrelated.

The data of long-range diffusion presented in Figure 1 have been obtained with zeolite crystals, whose radii are on the order of 10 μm, with root-mean-square displacements $\langle r^2(t)\rangle^{1/2}$ of the order of 100 μm. This allows us to base our consideration of the diffusion patterns on space units of 10 μm as schematically shown in Figure 1. The above-discussed prerequisite for the establishment of normal diffusion implies that molecular propagation from one of these space units to an adjacent one has to occur independently of the past of the molecule under consideration.

We shall demonstrate in the following that under the assumption of a low sticking probability, e.g., of as low as 10^{-7} as considered in ref 11, it is impossible to meet this requirement. As a consequence of this low sticking probability, molecules which have escaped from a crystallite have to remain in the intercrystalline space over very long intervals of time, before they will eventually be captured by a crystallite again (viz. after some 10^7 encounters with the outer surface of a crystallite). During this time, these molecules will traverse many space units of the type shown in Figure 1 and will cover, therefore, distances that are much larger than the crystallite size. By contrast, molecules being in the intracrystalline phase of such a space unit, will remain within this phase and, hence, also in the same space element, over relatively long time intervals, as an immediate consequence of the fact that the intracrystalline diffusivity D_{intra} is much smaller than the diffusivity in the intercrystalline space, D_{inter}. This means in particular that the propagation probability of molecules residing in a unit cell is notably determined by its past: those molecules, which have just entered, are most likely to leave the space unit in the next interval of time (since such a molecule is most likely to be a mobile one in the intercrystalline space), while those molecules which have resided in it for a while will continue to reside there, since these molecules most likely belong to the intracrystalline phase within the space element considered. In the given case, deviation from ordinary diffusion may be intuitively understood as the consequence of the diverging tendencies of the molecules inside and outside of the crystallites, effecting a narrower central part and a broader tailing of the propagator in comparison with a Gaussian.

Such a situation is incompatible with the experimental finding that the observed long-range diffusion follows the laws of ordinary diffusion. It has to be excluded, therefore, that during their lifetime in the considered space units the molecules are able to conserve their memory. This is only possible if molecular exchange between intracrystalline and intercrystalline space proceeds at a comparable, or even faster, rate than between the unit space elements. Since the extension of the space units is on the order of the mean free path in the Knudsen regime, at least after about each second collision with the crystallite surface, a molecule should be able to penetrate into the intracrystalline space. From this, a range between 0.5 and 1 appears to be the most probable range of sticking coefficients as compatible with the PFG NMR data on long-range diffusion of ethane in zeolite NaX.

With further systems, such as *n*-butane, *n*-heptane, and benzene in NaX,[24,31] water, methane, and ethane in silicalite-1/ZSM-5,[32] and ethane in NaCaA,[33] similar estimates are possible. In these cases, however, the lower limit of the sticking probability may be smaller, since in general for long-range diffusion studies crystallites smaller than those used in ref 16 have been applied. Therefore, considering comparable diffusion path lengths through the bed, the unit space elements may be chosen to contain notably more than one zeolite. As a consequence, on passing from space element to space element, the molecules more frequently collide with the external surface of the crystallites, so that for being captured by the intracrystalline space within one space element, a correspondingly lower sticking probability might be sufficient. In none of the considered cases, however, the sticking probability would drop notably below 0.1. For visualizing the way in which this new type of information is provided by the suggested mode of analyzing PFG NMR data under the regime of long-range diffusion, let us assume the opposite position, i.e., the conception of a very low sticking probability (e.g., 10^{-3} or lower). In this case, during the observation time t of the PFG NMR experiment one has to distinguish between essentially two groups of molecules. The first group consists of those molecules that have left the nanoporous particles and cover large distances within the bed of particles as a consequence of their low sticking probability. (Only after about 1000 or more encounters with the crystallite surface they would again be captured.) The other group is formed by the molecules that have remained inside the crystallites. Since the average propagator is simply the weighted sum of the propagators for these two groups, with eq 4 the spin−echo attenuation is expected to consist of two terms of the type of eq 6. The mean square displacement $\langle x^2(t)\rangle$ of the molecules within the particles is of the order of the particle radius or smaller. It is dramatically exceeded by the mean square displacement of those molecules, which have left the particles and cover, owing to their low sticking probability, very long

distances. Hence, due to the large value of $\langle x^2(t)\rangle$ in the exponent of eq 6, these molecules would cause an extremely rapid decay in the initial part of the attenuation curves. This initial part would be followed by a much slower signal attenuation due to the molecules that have remained within the individual crystallites. Their attenuation pattern would be given by eq 5 or eq 6, with a root-mean-square displacement by no way exceeding the crystal extension. Such a two-exponential behavior, however, is in strong contrast with the finding of long-range diffusion, where, as discussed above, the attenuation curves show essentially a single-exponential behavior for the root-mean-square displacement, which are only several times larger than the crystallite size. Therefore, the existence of such small sticking probabilities may definitely be ruled out.

3. Molecular Dynamics Simulations

The great success of molecular dynamics (MD) simulations in exploring the mechanisms of guest diffusion in nanoporous hosts[17,18,34−37] is going to be accomplished by first MD studies of molecular transport through the interface between the intracrystalline space and the surrounding gas phase.[19] In the present study we have re-analyzed the MD runs recently performed for simulating the adsorption/desorption kinetics of *n*-butane on aggregates of silicalite-1 with respect to their information on the sticking probability. Simultaneously, also the molecular escape probabilities from the intracrystalline space to the surrounding atmosphere have been considered.

The MD simulations of ref 19 were performed using a flexible atomic model[38] for an aggregate of the extensions $L_x = 3a$, $L_y = 2b$, and $L_z = 3c$ in the crystallographic *x*, *y*, and *z* directions. Terms *a*, *b*, and *c* denote the respective extensions of the unit cell.[39] The external surfaces perpendicular to the *x* and *z* directions exhibit half straight channels, with openings for the sinusoidal channels into these channels. The external surfaces perpendicular to the *y* direction are flat, with openings for the straight channels. In this model system, for the sake of simplicity, neither hydrogen nor hydroxyl groups are added to the external surface, which leads to deviation from a correct atomic coordinance at the surface. These deviations have to be considered to be of minor relevance for the obtained results.[19] The *n*-butane molecules were modeled by using the united atoms model,[40] with each CH_3 and CH_2 group simulated as one center of force. The site−site interaction was represented by truncated Lennard-Jones potentials with potential parameters following the data of ref 36. The interconnected dynamics of the host lattice and the guest molecules was determined by integrating the Newton's equation of motion using the Verlet velocity algorithm.[17,18] The trajectories were followed over 3×10^6 simulation steps with a time step of 1 fs. Rescaling molecular velocities ensured that a kinetic temperature of 300 K was maintained during the whole simulation runs. Further details of the simulations are described in ref 19.

Irrespective of the fact that, stimulated by industrial requirements, the production of zeolite nanocrystals is a timely challenge of zeolite sythesis,[41] the zeolite crystallites considered in these simulations are much smaller than those attainable for real experiments. The satisfactory agreement of the intracrystalline diffusivities resulting from these simulations with both PFG NMR data[12] and their (simulated) adsorption/desorption behavior[19] indicate, however, that any notable disturbance of the results by the finite size of the simulation box may be excluded.

The simulation runs to which we refer our considerations have been performed under the conditions as described by Table 2 of ref 19, viz., with an aggregate of silicalite-1 whose initial loading is below the equilibrium concentration that would be maintained by the surrounding atmosphere of statistically distributed molecules. The ratio between the volumes of the zeolite aggregate and the surrounding atmosphere ranges from 11 to 2% for different runs. As an example, Figure 2 displays the uptake curve resulting from the simulations for the conditions as specified by case 6 of Table 2 of ref 19, i.e., an initially empty zeolite agglomerate with 100 molecules in the surrounding atmosphere.

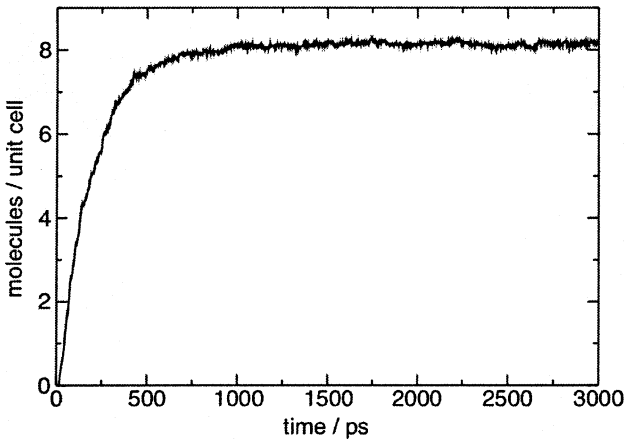

Figure 2. Typical uptake curve for *n*-butane on an aggregate of silicalite-1, resulting from the MD simulations[19] (case 6). In the presented example, dynamic equilibrium (last column of Table 1) is established after about 1.5 ns. The nonequilibrium data (filled symbols in Figure 4) have been determined before this time, the data of Table 1 and the equilibrium data of Figure 4 (open symbols) after this time.

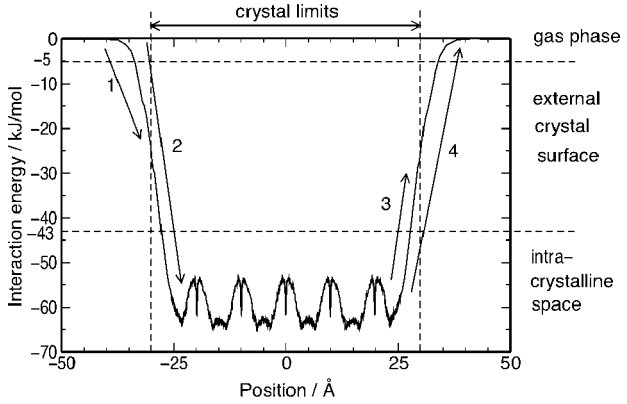

Figure 3. Profile of the potential energy of *n*-butane in silicalite-1 at 300 K along the *x* crystallographic direction of the aggregate[19] and classification of the elementary steps during molecular adsorption and desorption used for the calculation of the sticking and escape coefficients.

In ref 19, for the first time such curves have been derived from MD simulations. Further to the data presented in ref 19, for the present analysis we did also consider simulation runs leading to equilibrium concentrations of 1.7, 4.2, and 6.2 molecules per unit cell.

For analyzing the molecular sticking and escape probabilities, following the representation of the potential energy of the *n*-butane molecules in silicalite-1 (see reference[19] and our Figure 3), molecules with energies above −5 kJ/mol have been classified to be located in the gas phase. Molecules with energies between −5 and − 43 kJ/mol were attributed to the outer surface of the zeolite crystallites. Molecules with energies below − 43 kJ/mol are considered to be in the intracrystalline space. Though there is clearly some arbitrariness in these numbers,

TABLE 1: Numbers $n_{1(2,3,4)}$ of Elementary Events 1(2,3,4) during Molecular Adsorption and Desorption as Explained by Figure 3 and Resulting Sticking and Escape Probabilities (Coefficients) α and β

loading (molec/cc)	n_1	n_2	a	n_3	n_4	b	time (ns)
0.83	0	0	-	2	0	0	7.5
1.7	8	4	0.50	34	1	0.029	22.5
3.3	4	4	1	45	0	0	7.5
4.2	1	1	1	31	1	0.032	7.5
5.0	12	9	0.75	117	1	0.0085	15
6.2	11	5	0.45	112	3	0.026	7.5
6.6	17	10	0.59	138	6	0.0434	7.5
8.1	202	115	0.57	1880	104	0.055	30
9.0	206	95	0.46	1140	95	0.083	7.5
9.4	459	177	0.39	1642	179	0.109	7.5
10.3	234	61	0.26	1107	64	0.058	1.5

[a] Only those parts of the MD runs have been considered which took place under dynamic equilibrium (duration as indicated by last column).

their variation within reasonable limits will in no way affect the general message of the simulations.

Figure 3 schematically represents four different events of molecular propagation, which are closely related to the molecular sticking and escape probabilities, viz. (1) molecule from gas-phase encounters surface; (2) molecule from gas-phase enters intracrystalline space; (3) molecule from intracrystalline space gets to surface; (4) molecule from intracrystalline space enters gas phase.

Denoting by n_i the number of events of type i ($i = 1, 2, 3, 4$), the sticking probability α and the escape probability β are defined by

$$\alpha = n_2/n_1 \tag{9}$$

$$\beta = n_4/n_3 \tag{10}$$

The quantities α and β are likewise referred to as the sticking and escape coefficients, respectively. Table 1 summarizes the numbers of the different events relevant for the determination of the sticking and escape probabilities. All data have been determined from those parts of the simulation runs, where dynamic equilibrium has been established. The last column indicates the simulation time under equilibrium conditions. As the most prominent result of the analysis of the MD runs presented in Table 1, the sticking coefficients α are found to be of the order of magnitude as predicted from the PFG NMR studies of long-range diffusion in beds of zeolite crystallites, viz. within the range of the maximum possible value of $\alpha = 1$ and 1 order of magnitude smaller. At the same time, the data presented in Table 1 visualize the problems with simulations involving both the adsorbate and the surrounding gas phase. Owing to the huge differences in the respective concentrations under equilibrium, in the time scale of the simulations molecular exchange between both phases are extremely rare events, giving rise to rather poor statistics. As a consequence, only quite recently the consideration of such phenomena has become a topic of MD simulations,[19,42,43] and the deficiency in statistics appears in the scattering of the data as presented by Table 1 and Figure 4.

In addition to their order-of-magnitude agreement with the conclusions drawn from PFG NMR, there are three further items that underline the consistency of the MD results with respect to their message on the molecular sticking probabilities. (i) The probability that molecular encounters from the gas phase will be reversed is expected to increase with the probability that sites on the outer surface are already occupied by other molecules.

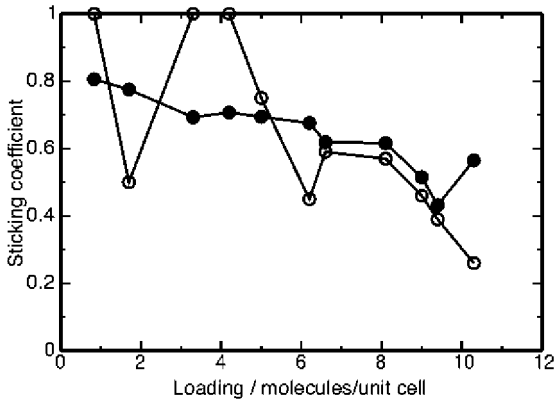

Figure 4. Sticking coefficients of *n*-butane on silicalite-1 at 300 K as a function of the loading, determined from MD simulations[19] under dynamic equilibrium (open symbols) and under transient conditions (filled symbols)

The decrease of the sticking coefficients with increasing loading is in complete agreement with this perception. (ii) Under dynamic equilibrium, the total numbers of molecules leaving and encountering the crystallites have to coincide. This means that n_4 has to be on the order of n_2. Again, disregarding the poor statistics, this coincidence is nicely reflected by the respective data given in Table 1. Using the same perspective, the large difference between the escape and the sticking probabilities may be understood as a simple correspondence to the large differences in the concentrations of the molecules in the adsorbed and gaseous phases. (iii) Since the propagation of a molecule on encountering the crystal surface should primarily be determined by the molecules and lattice atoms in its immediate vicinity rather than by the state of the whole system, it is very unlikely that the sticking coefficients obtained under dynamic equilibrium (as presented in Table 1) deviate notably from those determined under transient conditions. Hence, Figure 4 also displays the sticking coefficients determined during the initial phase of the MD runs, where dynamic equilibrium was not yet established. These data confirm the sticking coefficients determined under equilibrium conditions. Moreover, since they refer to longer simulation times, with much higher gaseous concentration, they notably improve the statistics.

4. Conclusion

For the first time, PFG NMR data referring to the regime of long-range diffusion and MD simulations comprising model zeolite particles with their surroundings have been explored with respect to the information provided by them about the elementary process of molecular passage through the interface between nanoporous materials, notably zeolites, and the surrounding atmosphere. The evidence of the PFG NMR diffusion studies is based on the fact that, under the conditions of long-range diffusion the probability distribution of molecular displacements, the so-called propagator, is governed by a Gaussian. Such a result implies fast molecular exchange between different crystallites during the observation time. This fact, combined with the information about the crystallite size, the mean distance of long-range diffusion, and the observation time, may be used for an estimate of the sticking probability. In MD simulations, from recording thousands of individual trajectories, the sticking probability is simply taken from counting the cases in which, after encountering the crystallite surface from outside, the molecules continue their trajectory in the interior of the crystallites.

By either route, substantial evidence is provided that, on encountering the surface from the gas phase, molecules will be captured by the nanoporous material with a probability close to 1. In this way, for the first time, direct information about the sticking coefficients on nanoporous materials is provided. The sticking coefficients are found to be larger by about 6 orders of magnitude than the only values which so far have been communicated in the literature and which have been deduced in an indirect way from the analysis of uptake experiments.

Sticking coefficients are technical key parameters for the quantification of the contact between the nanoporous material and the surrounding atmosphere in heterogeneous catalysis and mass separation. Simultaneously, they describe an important detail of molecular trajectories at the interface between the adsorbed and gaseous phases, reflecting quite general features of matter interaction. Further development in the field has most likely to focus on an improvement of the statistics in the simulations and on a more accurate modeling of the diffusion phenomena relevant for long-range diffusion in the PFG NMR studies, including surface modification of the nanoporous materials in order to ensure a deliberate variation of their sticking properties and an extension of the observation range of the diffusion phenomena including quasi-elastic neutron scattering [44] and solid-state NMR,[45] enabling the determination of exchange rates between adjacent adsorption sites. Such work is in progress.

Acknowledgment. Financial support by CNRS, DFG (grant KA 953/19-1 and international research training group "Diffusion in Porous Media"), and Fonds der Chemischen Industrie are gratefully acknowledged.

References and Notes

(1) Auerbach, S. M.; Carrado, K. A.; Dutta, P. K. *Handbook of Zeolite Science and Technology*; Marcel Dekker: New York, 2003.

(2) Ertl, G.; Knötzinger, H.; Weitkamp, J. *Handbook of Heterogeneous Catalysis*; Wiley-VCH: Chichester, 1997.

(3) Schüth, F.; Sing, K. S. W.; Weitkamp, J. *Handbook of Porous Solids*; Wiley-VCH: Weinheim, 2002.

(4) Ashmore, P. G. *Catalysis and Inhibition of Chemical Reactions*; Butterworth: London, 1963.

(5) Trapnell, B. M. W. *Chemisorption*; Butterworth: London, 1964.

(6) Tsai, M.-H. *Comput. Phys. Commun.* **2002**, *147*, 130.

(7) Tsuruta, T.; Tanaka, H.; Masuoka, T. *Heat Mass Transfer* **1999**, *42*, 4107.

(8) Matsumoto, M. *Fluid Phase Equilib.* **1998**, *144*, 307.

(9) Matsumoto, M.; Yasuoka, K.; Kataoka, Y. *Fluid Phase Equilib.* **1995**, *104*, 431.

(10) Nagayama, G.; Tsuruta, T. *J. Chem. Phys.* **2003**, *118*, 1392.

(11) Tanaka, H.; Zheng, S.; Jentys, A.; Lercher, J. A. *Stud. Surf. Sci. Catal.* **2002**, *142*, 1619.

(12) Kärger, J.; Ruthven, D. M. *Diffusion in Zeolites and Other Microporous Solids*; Wiley & Sons: New York, 1992.

(13) Kimmich, R. *NMR Tomography, Diffusometry, Relaxometry*; Springer: Berlin, 1997.

(14) Callaghan, P. T. *Principles of NMR Microscopy*; Clarendon Press: Oxford, 1991.

(15) Kärger, J.; Spindler, H. *J. Am. Chem. Soc.* **1991**, *113*, 7571.

(16) Geier, O.; Vasenkov, S.; Kärger, J. *J. Chem. Phys.* **2002**, *117*, 1935.

(17) Haberlandt, R.; Fritzsche, S.; Vörtler, H. L. In *Simulation of Microporous Systems: Confined Fluids in Equilibrium and Diffusion in Zeolites*; H. S. Nalwa, Ed., 2001; pp 357−443.

(18) Theodorou, D. N.; Snurr, R. Q.; Bell, A. T. In *Molecular Dynamics and Diffusion in Microporous Materials*; Alberti, G., Bein, T., Eds.; Pergamon Press: Oxford, U.K., 1996; pp 507−548.

(19) Simon, J.-M.; Decrette, A.; Bellat, J.-B.; Salazar, J. M. *Mol. Sim.* **2004**, *30*, 621.

(20) Simon, J.-M.; Kjelstrup, S.; Bedeaux, D.; Hafskjold, B. *J. Phys. Chem. B* **2004**, *2004*, 7186.

(21) Kärger, J.; Heink, W. *J. Magn. Reson.* **1983**, *51*, 1.

(22) Cotts, R. M. *Nature* **1991**, *351*, 443.

(23) Feller, W. *An Introduction to Probability Theory and its Applications*; John Wiley: New York, 1970.

(24) Kärger, J.; Kocirik, M.; Zikanova, A. *J. Colloid Interface Sci.* **1981**, *84*, 240.

(25) Kärger, J.; Pfeifer, H. *J. Chem. Soc., Faraday Trans.* **1991**, *87*, 1989.

(26) Kärger, J.; Pfeifer, H. In *NMR Studies of Molecular Diffusion, in: NMR Techniques in Catalysis*; Pines, A., Bell, A., Eds.; Marcel Dekker: New York, 1994; p 69.

(27) Rittig, F.; Coe, C. G.; Zielinski, J. M. *J. Am. Chem. Soc.* **2002**, *124*, 5264.

(28) Rittig, F.; Coe, C. G.; Zielinski, J. M. *J. Phys. Chem. B* **2003**, *107*, 4560.

(29) Rittig, F.; Farris, T. S.; Zielinski, J. M. *AICHE J.* **2004**, *50*, 589.

(30) Ardelean, I.; Mattea, C.; Farrher, G.; Wonorahardjo, S.; Kimmich, R. *J. Chem. Phys.* **2003**, *119*, 10358.

(31) Lorenz, P.; Bülow, M.; Kärger, J. *Colloids Surf.* **1984**, *11*, 353.

(32) Caro, J.; Bülow, M.; Jobic, H.; Kärger, J.; Zibrowius, B. *Adv. Catal.* **1993**, *39*, 351.

(33) Kärger, J.; Bülow, M.; Millward, B. R.; Thomas, J. H. *Zeolites* **1986**, *6*, 146.

(34) Demontis, P.; Gonzalez, J. G.; Suffritti, G. B.; Tilocca, A. *J. Am. Chem. Soc.* **2001**, *123*, 5069.

(35) Yang, J. H.; Clark, L. A.; Ray, G. J.; Kim, Y. J.; Du, H.; Snurr, R. Q. *J. Phys. Chem. B* **2001**, *105*, 4698.

(36) Vlugt, T. J. H.; Krishna, R.; Smit, B. *J. Phys. Chem. B* **1999**, *103*, 1102.

(37) Dubbeldam, D.; Smit, B. *J. Phys. Chem. B* **2003**, *107*, 12138.

(38) Ermoshin, V. A.; Smirnov, K. S.; Bougeard, D. *Chem. Phys.* **1996**, *202*, 53.

(39) Baerlocher, C.; Meier, W. M.; Olson, D. H. *Atlas of Zeolite Framework Types*; Elsevier: Amsterdam, 2001.

(40) Ryckaert, J. P.; Bellemans, A. *Faraday Discuss. Chem. Soc.* **1978**, *66*, 95.

(41) Mintova, S.; Metzger, T. H.; Olson, N. H.; Prokesova, P.; Bein, T. In *Abstracts and Full Papers of Plenary and Keynote Lectures of the 14th International Zeolite Conference*; van Steen, E., Callanan, L. H., Claeys, M. Eds.; Document Transformation Technologies: Cape Town, 2004; pp 125−126.

(42) Chandross, M.; Webb, E. B.; Grest, G. S.; Martin, M. G.; Thompson, A. P.; Roth, M. W. *J. Phys. Chem. B* **2001**, *105*, 5700.

(43) Arya, G.; Maginn, E. J.; Chang, H. C. *J. Phys. Chem. B* **2001**, *105*, 2725.

(44) Jobic, H.; Kärger, J. Bee, M. *Phys. Rev. Lett.* **1999**, *82*, 4260.

(45) Favre, D. E.; Schaefer, D. J.; Auerbach, S. M.; Chmelka, B. F. *Phys. Rev. Lett.* **1998**, *81*, 5852.